nature chemistry

ARTICLES

https://doi.org/10.1038/s41557-020-00589-8

Check for updates

Manganese-catalysed divergent silylation of alkenes

Jie Dong[1,5], Xiang-Ai Yuan[2,5], Zhongfei Yan[1,3,5], Liying Mu[2,5], Junyang Ma[1], Chengjian Zhu[1,4] and Jin Xie[1]✉

Transition-metal-catalysed, redox-neutral dehydrosilylation of alkenes is a long-standing challenge in organic synthesis, with current methods suffering from low selectivity and narrow scope. In this study, we report a general and simple method for the manganese-catalysed dehydrosilylation and hydrosilylation of alkenes, with $Mn_2(CO)_{10}$ as a catalyst precursor, by using a ligand-tuned metalloradical reactivity strategy. This enables versatility and controllable selectivity with a 1:1 ratio of alkenes and silanes, and the synthetic robustness and practicality of this method are demonstrated using complex alkenes and light olefins. The selectivity of the reaction has been studied using density functional theory calculations, showing the use of an ^{i}PrPNP ligand to favour dehydrosilylation, while a JackiePhos ligand favours hydrosilylation. The reaction is redox-neutral and atom-economical, exhibits a broad substrate scope and excellent functional group tolerance, and is suitable for various synthetic applications on a gram scale.

Organosilicon compounds, with their unique physical and chemical characters, have been widely used in a range of modern industries[1,2], pharmaceuticals[3], organic synthesis[4] and high-performance material fields[5] (Fig. 1a). Because they are not naturally occurring, new synthetic methodologies for the catalytic formation of carbon–silicon (C–Si) bonds[6–9] can assist silicon chemistry and have gained considerable momentum in recent years. Selective silylation of alkenes with commercially available silanes is one of the most reliable strategies with which to produce divergent organosilanes, such as alkylsilanes, vinylsilanes and allylsilanes, by hydrosilylation and dehydrosilylation[10] (Fig. 1b). Although platinum-catalysed hydrosilylation of alkenes has already been a focus in industrial manufacturing, annually consuming 5.6 tonnes of platinum[11,12], transition-metal-catalysed dehydrosilylation, a process associated with alkene hydrosilylation, remains largely undeveloped[1,13–15]. After several decades of efforts with precious-metal catalysts[16–20], base-metal-catalysed dehydrosilylation has recently witnessed notable progress[21–23]. For example, the Nakazawa group[21] has successfully achieved iron-catalysed dehydrosilylation of tethered dienes lacking allylic C–H bonds, and Chirik and colleagues[22] have achieved an elegant cobalt-catalysed dehydrosilylation of aliphatic alkenes for the synthesis of allylsilanes. Catalytic dehydrosilylation of alkenes without external oxidants[24,25], however, still faces several major challenges. These include (1) the requirement for at least two equivalents of alkenes (one as a sacrificial hydrogen acceptor), (2) concomitant hydrosilylation side reactions along with dehydrosilylation and (3) narrow scope and unpredictable stereoselectivity. Furthermore, ligand-tuned, base-metal-catalysed controllable dehydrosilylation and hydrosilylation reactions of alkenes are still elusive.

Manganese is the third most abundant transition metal in the Earth's crust and is relatively environmentally friendly. In general, manganese-catalysed organic transformations exhibit satisfactory air and moisture tolerance as well as excellent functional group compatibility[26,27]. The exploration of manganese-catalysed silylation of alkenes promises to be an attractive solution to problems related to the high cost of platinum[28–35]. The pioneering work of Faltynek in 1983[29] demonstrated that manganese-catalysed hydrosilylation reactions of alkenes lead to a mixture of products, and dehydrosilylation is more challenged than hydrosilylation (Fig. 1c).

$Mn_2(CO)_{10}$ is commercially available and possesses a weak Mn–Mn bond (185 kJ mol^{-1})[36]. It can produce a manganese radical that can be used in a series of atom transfer reactions in organic synthesis[37–41]. In the case of silanes and alkenes, the result of such a reaction is a facile hydrosilylation[30]. Recent efforts to explore the nature of silanes have been renewed, but only sterically hindered silanes have been reported to exhibit moderate dehydrosilylation selectivity (up to 10:1) with styrenes[34]. The ligand effect in organometallic chemistry prompted us to consider suitable ligands to tune the metalloradical reactivity for divergent organic transformations, a subject that currently attracts little attention[41,42]. We realized this concept through the use of a relatively electron-rich bidentate ^{i}PrPNP ligand (**L12**), which promotes dehydrosilylation, while the relatively electron-deficient JackiePhos ligand (**L22**) facilitates hydrosilylation (Fig. 1d). With a developed ligand-tuned metalloradical reactivity strategy, highly selective manganese-catalysed dehydrosilylation and hydrosilylation of alkenes can be controlled by different ligands. This will enrich manganese-catalysed radical transformations and assist in the synthesis of diverse organic silicon compounds.

Results and discussion

Reaction development. We began our study of the influence of ligands with the reaction of *p*-methylstyrene (**1a**) with triethylsilane (**2a**). As shown in Table 1, the model reaction can occur in the absence of ligand, but the hydrosilylation reaction is found to

[1]State Key Laboratory of Coordination Chemistry, Jiangsu Key Laboratory of Advanced Organic Materials, Chemistry and Biomedicine Innovation Center (ChemBIC), School of Chemistry and Chemical Engineering, Nanjing University, Nanjing, China. [2]School of Chemistry and Chemical Engineering, Qufu Normal University, Qufu, China. [3]College of Chemistry and Chemical Engineering, Anyang Normal University, Anyang, China. [4]College of Chemistry and Molecular Engineering, Zhengzhou University, Zhengzhou, China. [5]These authors contributed equally: Jie Dong, Xiang-Ai Yuan, Zhongfei Yan, Liying Mu. ✉e-mail: xie@nju.edu.cn

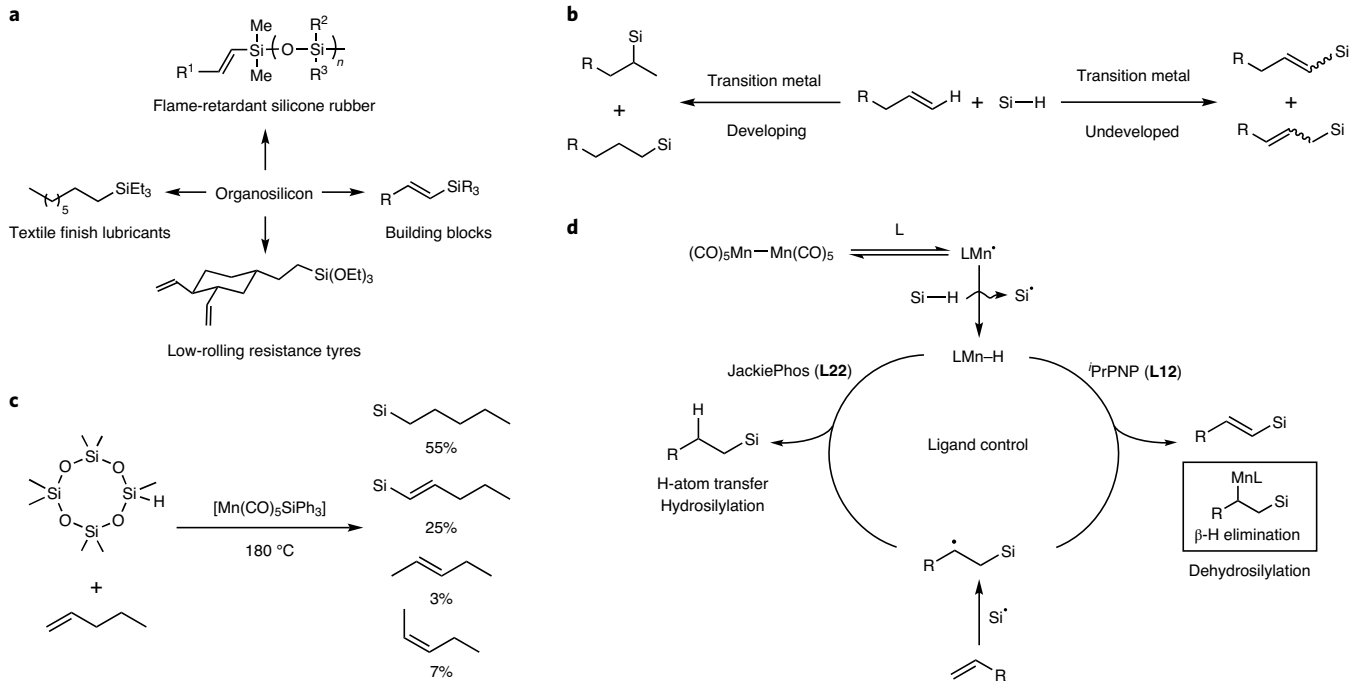

Fig. 1 | The state of the art for divergent silylation of alkenes. a, The organosilicons are important chemicals in industry, pharmaceuticals and high-performance material fields, as well as organic chemistry. Alkylsilanes and vinylsilanes are widely applied in textile finishing lubricants, silicone rubber, low-rolling-resistance tyres and as versatile building blocks in synthetic chemistry. **b**, The state of the art for transition-metal-catalysed dehydrosilylation and hydrosilylation. Transition metals Pt, Fe, Co, Ir, Ni, Mn and so on have been developed for hydrosilylation, and transition metals Ru, Ir, Rh, Re, Fe, Co and so on have been applied for dehydrosilylation. Despite recent advances, base-metal-catalysed dehydrosilylation remains undeveloped and still faces several major problems, such as low selectivity, sacrificial olefins or narrow scope. **c**, The seminal work of manganese-catalysed alkene hydrosilylation with heptamethylcyclotetrasiloxane, along with dehydrosilylation and alkene isomerization, where the hydrosilylation is more favoured than dehydrosilylation at 180 °C (ref. [29]). **d**, This work: manganese-catalysed divergent silylation of feedstock alkenes is achieved through ligand-tuned metalloradical activity, where ^{i}PrPNP ligand **L12** promotes dehydrosilylation while the JackiePhos ligand (**L22**) facilitates hydrosilylation.

be the predominant reaction (47% versus 10%), in accord with Faltynek's early report[29]. Because nitrogen-containing ligands such as terpyridine (**L1**) and bis(imino)pyridine (**L2**) have been applied in base-metal catalysis[22,33,35,43], we first focused our attention on screening a library of nitrogen-based ligands. It was found that terpyridine (**L1**) cannot promote either reaction, but bis(imino) pyridine (**L2**) could improve the hydrosilylation reaction, albeit with a lower total yield (**3a:4a** = 1:19). Continued screening of a series of N-based ligands indicated that the concept of ligand-tuned dehydrosilylation was realizable, as **L6** can improve the reaction selectivity to 3:1 (**3a:4a**). We rationalized that nitrogen-containing ligands (**L3**–**L6**) might deactivate the manganese catalytic reactivity. A first attempt with a traditional monophosphine ligand, triphenylphosphine (**L7**), supported our assumption and changed the reaction product distribution, with the hydrosilylation reaction dominating. To achieve manganese-catalysed dehydrosilylation, one urgent challenge is thorough suppression of hydrosilylation and promotion of dehydrosilylation.

Fortunately, with **L8** as the ligand, dehydrosilylation proceeds rather than hydrosilylation, increasing the selectivity of **3a:4a** to >5:1, although the reaction is slow. Among several bidentate ligands (**L8**–**13**, **L15** and **L16**), ^{i}PrPNP (**L12**) is the most effective. It can furnish the dehydrosilylation product (**3a**) in 85% gas chromatography (GC) yield with excellent stereoselectivity (E/Z > 99:1 determined by GC analysis). The use of electron-rich monodentate ligand **L14** resulted in only a small amount of desired dehydrosilylation product (**3a**) and the hydrosilylation process was inhibited. During ligand screening, it was also found that both the electronic and steric effects of phosphine ligands were crucial to manganese-catalysed hydrosilylation (**L17**–**L21**). This led us to examine JackiePhos (**L22**), a relatively electron-deficient and sterically hindered biaryl phosphine ligand[44], which with 3 mol% $Mn_2(CO)_{10}$ as catalyst, can improve the yield and selectivity of hydrosilylation to 79% and produce a **3a:4a** ratio of 3:79.

Mechanistic studies. We attempted to understand the unique ligand effects of ^{i}PrPNP and JackiePhos in manganese-catalysed divergent silylation. As illustrated in Fig. 2a, it was found that an air-stable Mn–H intermediate, **L12**$Mn(CO)_3H$ (**5**), can be isolated as a yellow powder in 60% yield from a reaction mixture containing the ^{i}PrPNP ligand (**L12**), $Mn_2(CO)_{10}$ and silanes, while other ligands such as **L8** or **L22** produced very little Mn–H complex. This indicates that different ligands can affect the reactivity and stability of the manganese intermediate. In all cases, $LMn(CO)_3SiEt_3$ intermediates were not obtained. An X-ray crystallographic structure analysis showed that the P–Mn–P angle (β) of the ^{i}PrPNPMn–H intermediate **L12**$Mn(CO)_3H$ (**5**) is indeed as low as 70.1° and the P–P distance in **5** is shorter than that in **L8**$Mn(CO)_3Br$ (**6**) (2.579 versus 2.706 Å).

When the isolated Mn–H intermediate **L12**$Mn(CO)_3H$ (**5**) was used as a manganese precursor, an 89% yield of **3a** was obtained, but the reaction of $Mn(CO)_5SiEt_3$ with the **L12** combination resulted in only traces of product (Fig. 2b). These experimental results imply that the Mn–H intermediate **L12**$Mn(CO)_3H$ (**5**) may be an important component in the catalytic cycle. Deuterium labelling experiments (Fig. 2c) show that both β-H elimination and Si–H cleavage may not be involved in the rate-limiting steps for dehydrosilylation, but Si–H cleavage (kinetic isotope effect (KIE) = 4.94) would be the

Table 1 | Discovery of reaction conditions

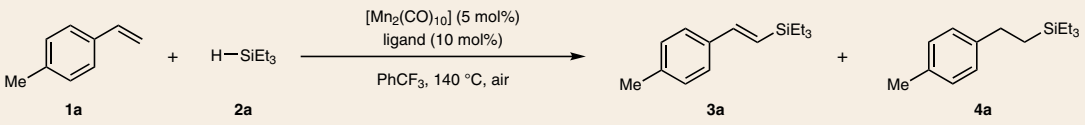

No ligand
3a: 10%
4a: 47%

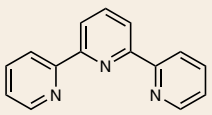

L1
3a: ND; **4a**: ND

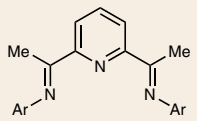

L2 Ar = 2,4,6-trimethylphenyl
3a: 1%; **4a**: 19%

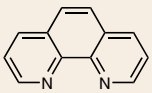

L3
3a: ND; **4a**: ND

L4 R = H, **3a**: <1%, **4a**: <1%
L5 R = *2*-Me, **3a**: <1%, **4a**: <1%
L6 R = 3-COOEt, **3a**: 5%, **4a**: 1.5%

L7
3a: 5%; **4a**: 10%

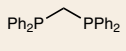

L8
3a: 5%; **4a**: <1%

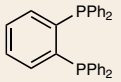

L9
3a: 6%; **4a**: <1%

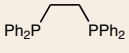

L10
3a: 9%; **4a**: <1%

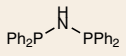

L11
3a: <1%; **4a**: <1%

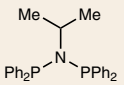

L12
3a: 85%; **4a**: ND

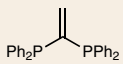

L13
3a: 5%; **4a**: ND

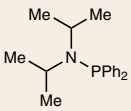

L14
3a: 2%; **4a**: ND

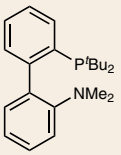

L15
3a: 20%; **4a**: 69%

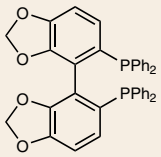

L16
3a: <1%; **4a**: 9%

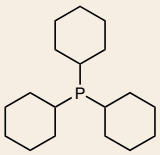

L17
3a: 3%; **4a**: 35%

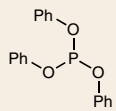

L18
3a: 3%; **4a**: 57%
3a: 12%[a]; **4a**: 80%[a]

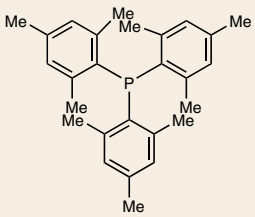

L19
3a: 4%[a]; **4a**: 55%[a]

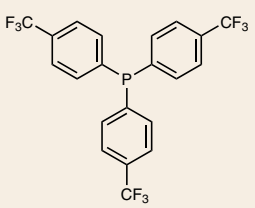

L20
3a: 5%[a]; **4a**: 43%[a]

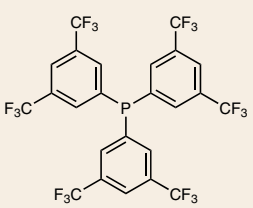

L21
3a: 3%[b]; **4a**: 62%[b]
3a: 4%[c]; 4a: 59%[c]

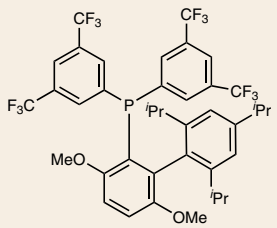

L22
3a: 2%[b], **4a**: 67%[b]
3a: 3%[c], **4a**: 79%[c]

Unless otherwise noted, the reaction conditions are $Mn_2(CO)_{10}$ (5 mol%), ligand (10 mol%), **1a** (1.0 mmol), **2a** (1.0 mmol), 140 °C, $PhCF_3$ (0.2 ml), 24 h. [a]$Mn_2(CO)_{10}$ (5 mol%), ligand (10 mol%), **1a** (1.0 mmol), **2a** (1.0 mmol), 120 °C, $PhCF_3$ (0.2 ml), 24 h. [b]$Mn_2(CO)_{10}$ (5 mol%), ligand (5 mol%), **1a** (1.0 mmol), **2a** (1.0 mmol), 120 °C, $PhCF_3$ (0.2 ml), 24 h. [c]$Mn_2(CO)_{10}$ (3 mol%), ligand (6 mol%), **1a** (1.0 mmol), **2a** (1.0 mmol), 120 °C, $PhCF_3$ (0.2 ml), 24 h. GC yield was used during reaction conditions optimization. ND, not detected.

rate-limiting step for hydrosilylation. This also demonstrates that the hydrogen atom in the hydrosilylation of alkenes originates from the silanes. As shown in Fig. 2d, using different ligands leads to a completely different total reaction profile. For dehydrosilylation, the reaction rate in the initial phase is very fast, but then becomes slow, possibly due to catalyst deactivation. We speculated that the fast dehydrosilylative process in the initial period could promptly decrease the substrate concentration to ensure good dehydrosilylative selectivity. The hydrosilylation rate, on the other hand, is relatively smooth, with ~20% yield of **4a** formed after 3 h. This significant difference in reaction rate further demonstrates the important role of ligands in divergent silylation. We also investigated both dehydrosilylation and hydrosilylation using different *para*-substituted styrenes. The Hammett plot ($\log(k/k_0)$ versus σ_p) shows a linear relationship, with positive slope for both dehydrosilylation (0.5313) and hydrosilylation (0.8102) (Fig. 2d). This indicates that the electronic effect of the alkenes may not be a vital factor for manganese-catalysed dehydrosilylation and hydrosilylation.

On addition of 2,2,6,6-tetramethylpiperidinyloxy (TEMPO, a radical trapping reagent) into the model reaction with either **L12** or **L22**, dehydrosilylation and hydrosilylation are both inhibited, suggesting a likely radical pathway for both transformations (Fig. 2b). To further confirm this, a reaction mixture with **L12** and **L22**, after the addition of dimethyl pyridine *N*-oxide (DMPO) as a spin-trapping reagent, was subjected to electron paramagnetic resonance (EPR) analysis. The broad resonance signals in the resulting EPR spectra may be the result of superposition of several radicals with trapped manganese radical species (Supplementary Fig. 15). The adducts of DMPO with **L12**$(CO)_3Mn^{\bullet}$ and **L22**$(CO)_4Mn^{\bullet}$ were successfully identified by high-resolution mass spectrometry (HR-MS).

Proposed mechanism. A proposed mechanism can be derived from thermal cleavage of the Mn–Mn bond in ligand-coordinated carbonyl manganese (Fig. 3a). The reactive manganese radical resulting from this cleavage undergoes a hydrogen atom transfer (HAT) process with a silane to generate the corresponding LMnH species and a silyl radical[34], which rapidly undergoes radical addition to olefins to furnish a secondary alkyl radical (**8**). The ^{i}PrPNP-bound Mn–H species can regenerate the corresponding manganese radical and extrusion of H_2 by thermal homolysis. The shuttle between **L12**Mn–H and **L12**$Mn^{\bullet}$ may support a very low concentration of **L12**$Mn^{\bullet}$, while the concomitant silyl radical successively adds to the olefins, increasing the concentration of the alkyl radical (**8**). When the concentration of the alkyl radical becomes much higher than the concentration of the corresponding **L12**$Mn^{\bullet}$, a dynamically controlled radical cross-coupling[34] of alkyl radical **8** and **L12**$Mn^{\bullet}$, guided by a 'persistent radical effect', takes place[45,46]. In our system, the ^{i}PrPNP-bound manganese radical would be more reactive and

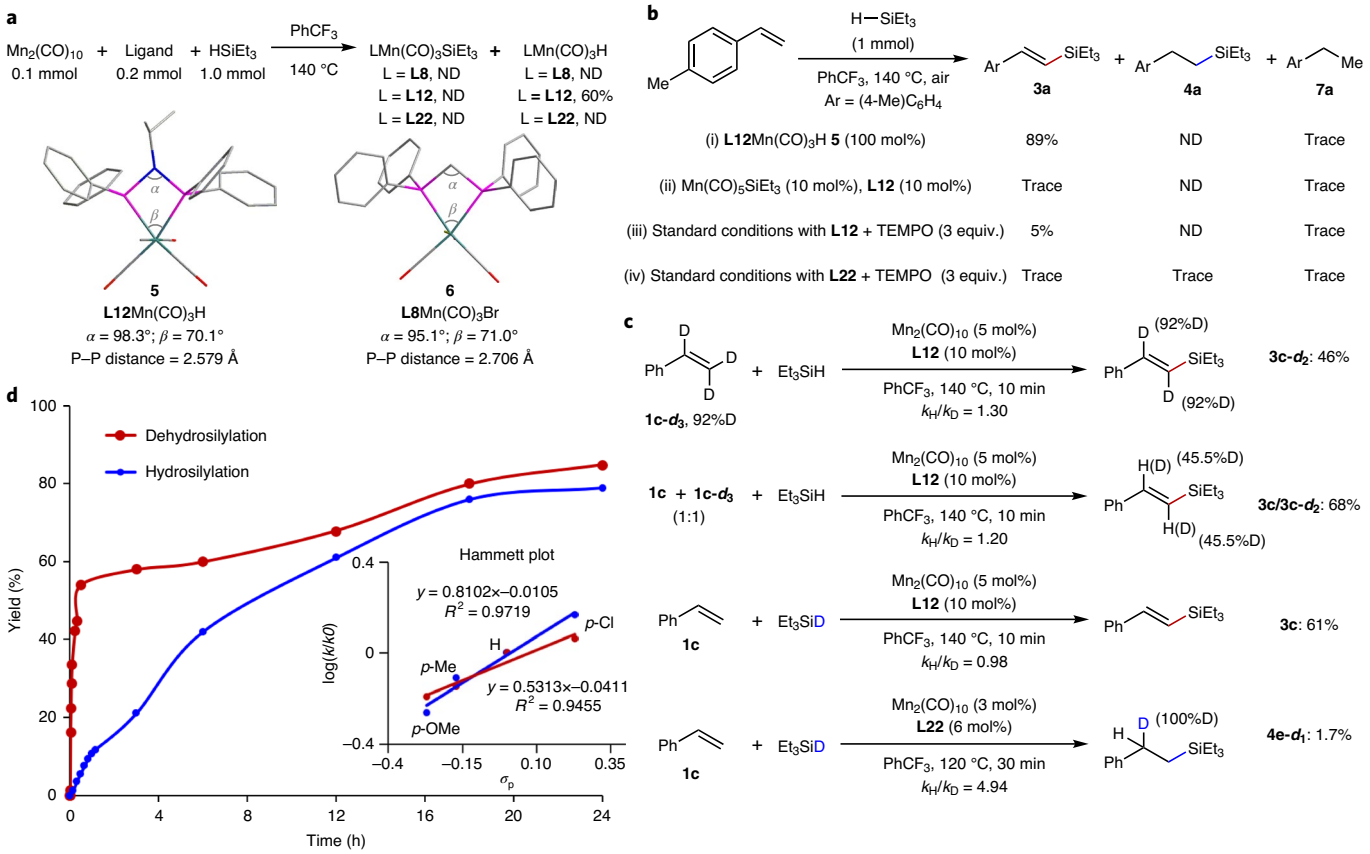

Fig. 2 | Preliminary mechanistic studies. a, Isolation and characterization of the **L**Mn–H intermediates. The **L12**$Mn(CO)_3H$ complex (**5**) is relatively air-stable, while **L8**$Mn(CO)_3$–H and **L22**$Mn(CO)_4$–H cannot be obtained. To compare the unique ligand skeleton effect in **L12**$Mn(CO)_3H$ (**5**), **L8**$Mn(CO)_3Br$ (**6**) was prepared (Supplementary Section 7.2). The X-ray structures of **5** and **6** (hydrogen atoms are omitted for clarity) are also shown. **b**, Mechanistic control experiments with GC yielded the following: (i) use of the **L12**$Mn(CO)_3H$ intermediate can successfully initiate dehydrosilylation, and only trace hydrogenation by-product **7a** was detected; (ii) use of $Mn(CO)_5SiEt_3$ resulted in failure; (iii) the addition of 3 equiv. TEMPO significantly inhibited dehydrosilylation; (iv) the addition of 3 equiv. TEMPO suppressed hydrosilylation. The experimental results for (iii) and (iv) indicate a radical mechanism. **c**, Deuterium labelling experiment. Parallel and competitive KIE experiments with D-labelled styrenes demonstrate that the β-H elimination process may not be the rate-determining step in dehydrosilylation. Si–H cleavage is also not involved in the rate-determining step for dehydrosilylation, but it would be the rate-limiting step for manganese-catalysed hydrosilylation. **d**, The total reaction profiles for the dehydrosilylation reaction (red) and hydrosilylation reaction (blue) of **1a** and **2a**, as well as the Hammett plot (small window) in one single experiment. We estimate the error in the integral ratios to be <1% based on the signal-to-noise ratio of the GC spectra. The reaction progress showcases that dehydrosilylation is faster than hydrosilylation in the initial phase. ND, not detected.

alkyl radical **8** appears to be less reactive. Because of the ligand effect of ^{i}PrPNP, the coupled alkylmanganese(I) intermediate (**9**) readily undergoes CO dissociation and *syn*-periplanar β-H elimination to afford the dehydrosilylation product (**3**). On the other hand, when the JackiePhos ligand is employed, the resulting alkyl radical (**8**) can undergo HAT with **L22**MnH species to give rise to the hydrosilylation product (**4**).

Computational selectivity studies. To better understand the origin of ligand-controlled selectivity, the key selectivity-controlled steps of dehydrosilylation and hydrosilylation with different ligands (**L12** and **L22**) were explored using density functional theory (DFT) calculations at the TPSSh-D3(BJ)/def2-TZVP//M06/def2-SVP level at the experimental temperature (140 °C for **L12**; 120 °C for **L22**). The primary results for the reaction of radical **8a**, the β-H elimination step affording dehydrosilylation product **3a** and the HAT process giving hydrosilylation product **4a** are depicted in Fig. 3b (the free energy profiles are provided in Supplementary Figs. 23 and 24).

For the ^{i}PrPNP ligand (**L12**), alkyl radical **8a** can couple with **L12**Mn$^{\bullet}$ to give alkylmanganese intermediate **9–L12**. We envisioned that the small bite angle of the ^{i}PrPNP ligand would enable its two phosphine atoms just medially distributed in the equator of **9-L12** and thus dissociation of one CO ligand might become relatively accessible to form **IN3–L12** possibly due to the *trans*-influence (Supplementary Fig. 26, CO dissociation energy in **9–L12**: 9.9 versus 12.8 and 31.8 kcal mol^{-1}). The following intermediate **IN3–L12** can undergo β-H elimination via transition state **TS3-L12** to produce the dehydrosilylation product **3a**. Alternatively, alkyl radical **8a** can interact with **L12**Mn–H to undergo the HAT process via transition state **TS4-L12**, which would deliver hydrosilylation product **4a**. However, the noncovalent interactions analyses for HAT transition state **TS4-L12** demonstrate that there is severe steric crowding between the skeletons of alkyl radical **8a** and ^{i}PrPNP ligand **L12**. Comparing the two pathways with ligand **L12**, the transition state for the formation of dehydrosilylation product **3a** is lower (23.9 kcal mol^{-1} via **TS3-L12**) than that of hydrosilylation product **4a** (27.9 kcal mol^{-1} via **TS4-L12**), which suggests that the dehydrosilylation pathway is kinetically more favourable than hydrosilylation for ligand **L12**.

For the JackiePhos ligand **L22**, although both energy barriers of the β-H elimination process and HAT process become smaller than that for **L12**, its HAT pathway via **TS4-L22** (18.5 kcal mol^{-1})

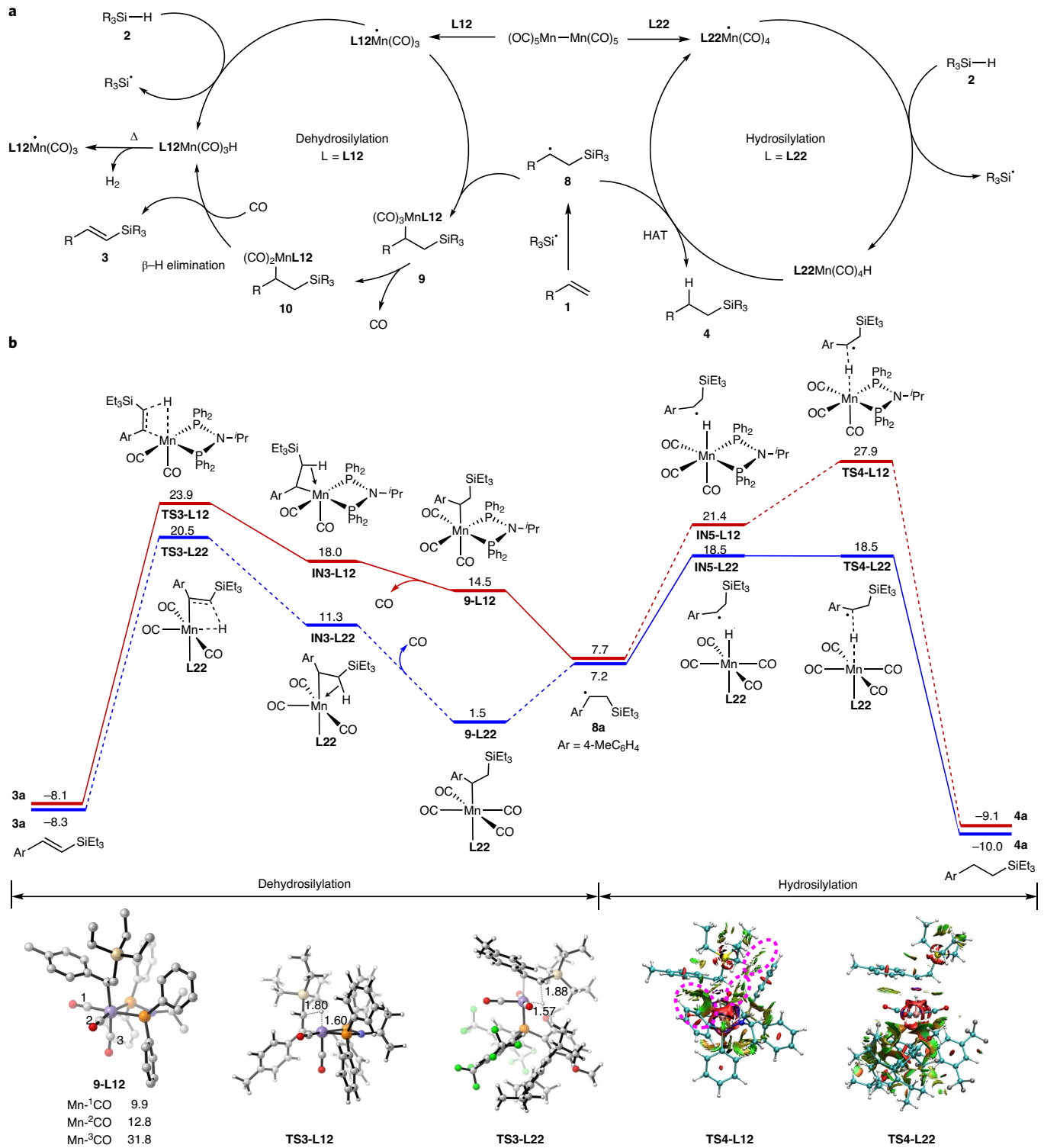

Fig. 3 | Mechanistic proposal and DFT studies. a, The proposed reaction mechanism. Ligand-coordinated carbonyl manganese is formed in situ. The β-H elimination process and the HAT process are the key steps to control dehydrosilylation and hydrosilylation selectivity. **b**, The calculated free energy profile of selectivity for different ligands at the reaction temperature (140 °C for **L12**; 120 °C for **L22**). The profiles start with **8a**, which is formed from **1a**, **2a** and **L**Mn•. The full profiles for both reactions, including steps for the formation of **8a**, are provided in the Supplementary Information (Supplementary Fig. 23 for **L12** and Supplementary Fig. 24 for **L22**). The computational results explain the difference in selectivity of the competitive reactions with different ligands; the preferred energy barrier for ^{i}PrPNP ligand (**L12**) is 23.9 kcal mol^{-1} and for the JackiePhos ligand (**L22**) is 18.5 kcal mol^{-1}. The CO dissociation free energies of **9–L12** are given in kcal mol^{-1} and bond distances of the transition states of **TS3-L12** and **TS3-L22** are given in Å. Noncovalent interaction analyses for the HAT transition states of **TS4-L12** and **TS4-L22** are shown: red, blue and green surfaces represent the steric effect, strong interaction and weak interaction, respectively. All energies are in kcal mol^{-1}.

Table 2 | Synthetic scope of ligand-controlled manganese-catalysed divergent silylation

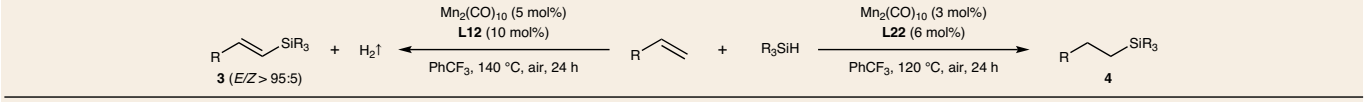

Styrenes

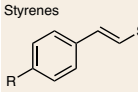

3a: R = Me, 76%
3b: R = ^{t}Bu, 82%
3c: R = H, 78%
3d: R = OMe, 73%
3e: R = F, 74%
3f: R = CN, 65%
3g: R = CF_3, 75%

3h: 77%

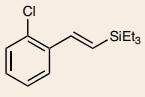

3i: 56%

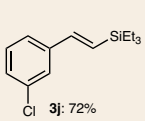

3j: 72%

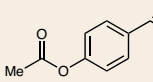

3k: 84%

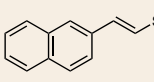

3l: 89%

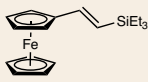

3m: 66%

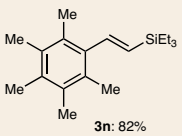

3n: 82%

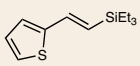

3o: 73%

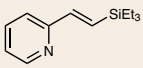

3p: 35%

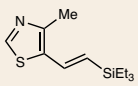

3q: 48%

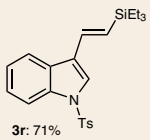

3r: 71%

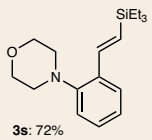

3s: 72%

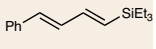

3t: 61%

Aliphatic alkenes

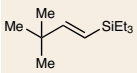

3u: 58%

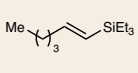

3v: 53%

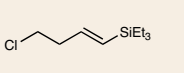

3w: 77%

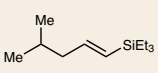

3x: 68%

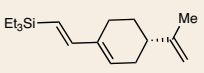

3y: 70%

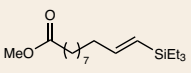

3z: 70%

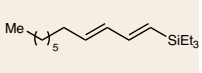

3aa: 76%

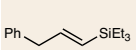

3ab

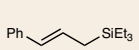

3ab'

69% (**3ab**:**3ab'** = 11: 89)

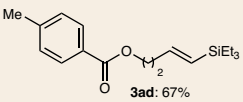

3ad: 67%

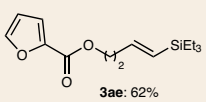

3ae: 62%

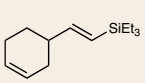

3af: 60%

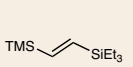

3ag: 71%

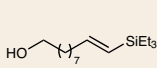

3ah: 50%

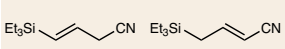

3ac

3ac'

77% (**3ac**:**3ac'** = 63:37)

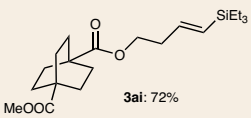

3ai: 72%

3aj: 54%

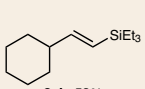

3ak: 53%

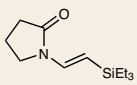

3al: 40%

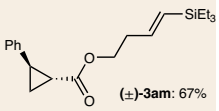

(±)-3am: 67%

Complex alkenes

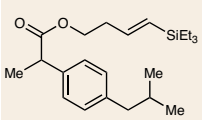

3an: 67% (from ibuprofen)

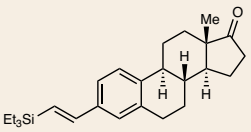

3ao: 45%[a,b] (from oestrone)

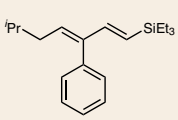

3ap: 83% (from cocal)

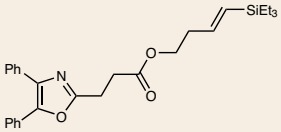

3aq: 56% (from oxaprozin)

3ar: 43% (from naproxen)

3as: 39%[a,b] (from adapalene)

3at: 43% (from pregnenolone)

3au: 46%[b] (from diacetone-D-glucose)

3av: 47%[a,b] (from allylestrenol)

Silanes

3aw: 79%

3ax: 65%

3ay: 70%

3az: 51%

3ba: 57%

3bb: 72%

3bc: 85%

3bd: 86%

3be: 85%

3bf: 87%

3bg: 31%

3bh: 49%

3bi: 87%

3bj: 73%

3bk: 77%

3bl: 38%

3bm: ND

3bn: ND

Hydrosilylation

R = H, **4a**: 83% (h:dh = 98:2)
R = Me, **4b**: 79% (h:dh = 96:4)
R = F, **4c**: 89% (h:dh = 95:5)

4d: 82%
h:dh >99:1

4e: 76%
h:dh = 98:2

4f: 50%[c]
h:dh = 95:5

4g: 86%
h:dh = 98:2

4h: 72%[d]
h:dh > 95:5[e]

4i: 89%[d]
h:dh > 95:5[e]

4j: 88%
h:dh = 95:5

4k: 85%
h:dh = 99:1

4l: 81%
h:dh > 99:1

4m: 76%

Unless otherwise noted, the optimized conditions are as described in Table 1 for dehydrosilylation and hydrosilylation in 1 mmol scale. The stereoselective ratio (*E*/*Z*) represents the ratio of (*E*)-vinylsilanes to (*Z*)-vinylsilane, as determined by ^{1}H NMR analysis of isolated products. The h:dh values represent the ratio of product **4** to **3** as determined by GC analysis. [a]The reaction was performed at 160 °C. [b]The reaction time was 30–36 h. [c]The reaction was performed at 110 °C. [d]The reaction was performed at 140 °C for 30 h. [e]The h:dh ratios were determined by ^{1}H NMR analysis of isolated products. Ts, toluenesulfonyl; Et, ethyl; Pr, propyl; Cy, cyclohexanyl; Bn, benzyl; ^{t}Bu, *tert*-butyl; Ad, 1-adamantyl.

a

Light alkene	Conditions A: Product	Yield	Selectivity	Conditions B: Product	Yield	Selectivity
Ethylene	 **4n**	40%	99:1	 **4n**	90%	99:1
Propylene	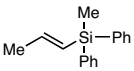 **3bo**	40%	>99:1	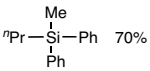 **4o**	70%	>99:1
Propylene	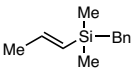 **3bp**	75%	>99:1	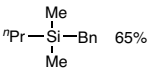 **4p**	65%	91:9
Butylene	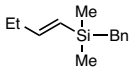 **3bq**	51%	>99:1	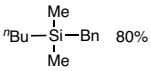 **4q**	80%	>99:1

b

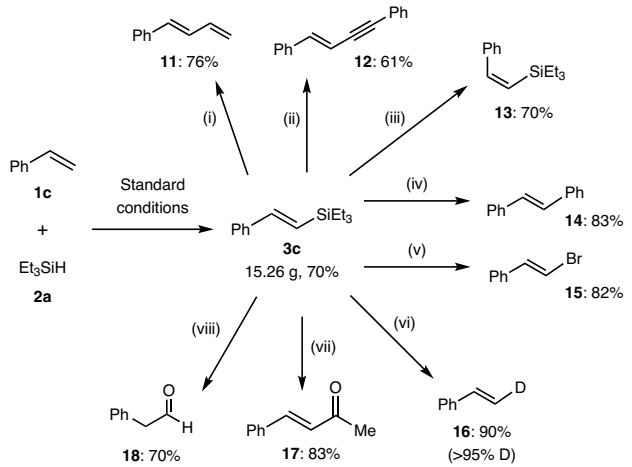

Fig. 4 | Enrichment and elaboration of products. a, Divergent silylation with light olefin. Conditions A: $Mn_2(CO)_{10}$ (5 mol%), **L12** (10 mol%), alkene (0.2–0.5 MPa), silane (1–3 mmol), 115–120 °C, $PhCF_3$ (5.0 ml), 24 h. Conditions B: $Mn_2(CO)_{10}$ (5 mol%), **L21** (5 mol%), alkene (0.2–0.4 MPa), silane (1–4 mmol), 130 °C, $PhCF_3$ (5 ml), 24 h. The product selectivities for dehydrosilylation and hydrosilylation were determined by GC analysis. **b**, The 100 mmol scaled-up experiment under standard reaction conditions to afford product **3c** and its downstream diversification. To prepare product **11**: (i) $Pd(OAc)_2$ (10 mol%), **3c** (0.5 mmol), bromoethene (2.5 mmol), tetrahydrofuran (THF), 150 °C, 24 h. To prepare product **12**: (ii) $Pd(OAc)_2$ (10 mol%), **3c** (0.5 mmol), (iodoethynyl) benzene (1.5 mmol), THF, room temperature, 24 h. To prepare product **13**: (iii) **3c** (1 mmol), $Ir(ppy)_2(dtbpy)PF_6$ (4 mol%), blue LEDs (2 × 45 W), CH_3CN, 30 h. To prepare product **14**: (iv) $Pd(dba)_2$ (10 mol%), **3c** (0.5 mmol), Ph–I (1.5 mmol), Bu_4NF (1 M in THF, 1.5 mmol), THF, room temperature, 1 h. To prepare product **15**: (v) **3c** (0.5 mmol), Br_2 (1.5 mmol), hexane, room temperature, 12 h. To prepare product **16**: (vi) **3c** (2 mmol), D–Cl (6 mmol), CH_3CN, 60 °C, 24 h. To prepare product **17**: (vii) $AlCl_3$ (3 mmol), **3c** (1 mmol), CH_3COCl (1.5 mmol), CH_2Cl_2, room temperature, 3 h. To prepare product **18**: (viii) $Pd(OAc)_2$ (10 mol%), **3c** (0.5 mmol), $PhI(OAc)_2$ (0.5 mmol), AcOH (2 ml), 120 °C, 24 h. dba, bis(dibenzylideneacetone); ppy, 2-phenylpyridine; dtbpy, 2,2'-bis(4-*tert*-butylpyridine).

is lower in energy compared with its β-H elimination pathway via **TS3-L22** (20.5 kcal mol^{-1}). This makes the hydrosilylation kinetically more favourable than the dehydrosilylation process for ligand **L22** and thus it predominantly delivers hydrosilylation product **4a**. We speculated that the small steric effect would contribute to the preferred HAT process (Supplementary Fig. 28). The preferred barrier for ^{i}PrPNP ligand **L12** is 23.9 kcal mol^{-1} and that of JackiePhos ligand **L22** is 18.5 kcal mol^{-1}. These differences in the apparent barriers might reflect the variation of reaction temperature: 140 °C for dehydrosilylation with ligand **L12** and 120 °C for hydrosilylation with ligand **L22**. The calculated results are in agreement with the experimental observation of the product distribution (**3a** versus **4a**) with different ligands.

Synthetic scope. Owing to their unique reactivity and low toxicity, vinylsilanes are particularly attractive reagents in organic synthesis[4]. With the optimized conditions that have been established, a wide variety of structurally diverse vinylsilanes can be obtained from commercially available feedstocks by manganese-catalysed dehydrosilylation (Table 2). The readily available substrates, broad reaction scope, excellent functional group tolerance and good stereoselectivity (*E*:*Z* > 95:5) make this a general and practical candidate[47–49]. Using 1 mmol of alkene and 1 mmol of triethylsilane in an air atmosphere, all the styrenes are effective coupling partners, in spite of the electron and substituent effects at the *ortho*-, *meta*- and *para*-positions (**3a**–**3k**, **3n** and **3s**). The heteroaromatic and ferrocenyl alkenes tolerate the manganese-catalysed dehydrosilylation conditions well (**3m**, **3o**–**3r**). The synthetic advantages of the reaction are further illustrated by direct dehydrosilylation of non-activated aliphatic olefins (**3u**–**3am**), in which control of the regioselectivity (β-H versus β′-H elimination) remains a great challenge. For example, β′-H elimination occurs to generate allylsilanes with cobalt catalysis[22]. In manganese-catalysed dehydrogenative silylation of aliphatic alkenes, the regioselectivity (β-H versus β′-H elimination) is generally acceptable. A competing β′-H elimination occurs predominantly when aliphatic alkenes bear an acidic allylic C(sp^3)–H bond, such as a benzylic C–H bond and the α-C(sp^3)–H bond of nitrile (**3ab′**, **3ac′**). Because of the α-silicon effect[50] in the generated alkylmanganese intermediate (**10**), the acidity of the β-C(sp^3)–H bond adjacent to the silicon atom has been increased while the hydricity has been decreased compared with the competing β′-C(sp^3)–H bond. This may indicate that manganese-mediated β-H elimination prefers to occur at the relatively acidic β-C–H bonds, favouring the formation of vinylsilanes as the main product (**3v**–**3x**, **3z**, **3ad**–**3af**, **3ah**–**3ak**, **3am**, **3an**, **3aq**–**3as**, **3av**, **3bo**–**3bq**). The regio- and stereoselectivity in aliphatic alkenes further highlights the synthetic robustness for the catalytic chemistry of manganese. Moreover, when the substrate contains different alkene units, this protocol prefers to undergo dehydrosilylation at the less sterically hindered terminal double bonds (**3y**, **3af**). Conjugated 1,4-dienes can undergo manganese-catalysed dehydrosilylation smoothly and selectively to furnish products **3t**, **3y** and **3aa** with satisfactory yields. The alcohol-type alkenes (**3ah**) can still be successfully employed for dehydrosilylation under standard conditions, albeit with 13% yield of silyl-ether by-product (RO-$SiEt_3$). When terminal alkynes were employed instead of alkenes, no desired dehydrosilylation products were formed (Supplementary Fig. 30). Among those alkynes tested, they gave only a trace to a small amount of *Z*-selective hydrosilylation product (up to 15% yield). This may also indicate that the use of ^{i}PrPNP ligand **L12** would substantially change the reactivity of Mn–H species and render **L12**Mn–H unfavourable for the HAT process.

Focusing on synthetic practicability and robustness, we applied this method to dehydrosilylation of a series of complex alkenes (**3an**–**3av**), and demonstrated its ability to retain its valuable chemo-, regio- and stereoselectivity in addition to excellent functional group tolerance. Importantly, the introduction of reactive ketone moieties in the substrates minimally influences the

chemoselectivity of the reaction (**3ao**, **3at**). All the tertiary silanes (**3aw**–**3bl**), even the highly sterically hindered H–Si($SiMe_3$)$_3$ (**3ax**) are good coupling partners for dehydrosilylation. The alkoxysilanes (**3az**, **3bb** and **3bl**) and H–SiMe–($OSiMe_3$)$_2$ (**3bj**) also appear to be compatible. However, the primary and secondary silanes are currently challenging substrates for manganese-catalysed dehydrosilylation (**3bm** and **3bn**), possibly due to the difficulty to generate corresponding silyl radicals.

Another advantage of this protocol is the diverse synthetic potential of organosilicon compounds. Manganese-catalysed, highly selective hydrosilylation of alkenes can provide one powerful access to a library of alkylsilanes[51–55]. On changing ^{i}PrPNP **L12** to the JackiePhos **L22** ligand, a manganese-catalysed hydrosilylation reaction of alkenes has been achieved without the use of additional silanes (alkenes:alkenes = 1:1). Both aromatic and aliphatic alkenes can readily undergo hydrosilylation, furnishing a broad variety of alkylsilanes (**4a**–**4l**) in yields of up to 89% and with up to >99:1 selectivity. The reaction of polymethylhydrosiloxane and 1,2,4-trivinylcyclohexane (mixture of isomers) can also readily occur to furnish silicone (**4m**) in 76% yield. Importantly, for all the examples shown in Table 2, only the linear-selective hydrosilylation and dehydrosilylation products were obtained and no branched selectivity was observed. This would originate from the anti-Markovnikov addition of silyl radicals to alkenes.

Synthetic application. Subsequently, we investigated the challenging light olefins, such as ethylene, propylene and butylene, and the results are shown in Fig. 4a. With the exception of ethylene, light olefins can achieve ligand-tuned dehydrosilylation (**3bo**–**3bq**) and hydrosilylation (**4n**–**4q**) with moderate to good yields. With ethylene, only the hydrosilylation product (**4n**) was produced under any reaction conditions. We hypothesize that the resulting methylene radical intermediate may be too short-lived to undergo radical coupling with a manganese radical. The commercially abundant monophosphine ligand (**L21**) can, however, afford yields comparable to and as selective as JackiePhos (**L22**) in the hydrosilylation of gaseous alkenes. As shown in Fig. 4b, the reaction can be scaled up to 100 mmol, affording dehydrosilylation product **3c** in 70% yield (15.26 g). A series of useful building blocks (**11**–**18**) are also readily available through diversification of vinylsilanes, demonstrating the synthetic significance and utility of the reaction in organic synthesis. More importantly, it affords an attractive route to synthesize compounds such as hyacinthine (**18**) from inexpensive styrene through a silicon relay.

Conclusions

As a result of efforts to develop strategies for base-metal-catalysed diverse silylation of alkenes, a highly selective, scalable and general dehydrosilylation and hydrosilylation has been realized by ligand-tuned manganese-radical activity. Given the ubiquity and availability of alkenes and silanes, this new type of reaction can enable a series of powerful transformations of styrenes, aliphatic alkenes and light alkenes. The successful use of suitable ligands to achieve product diversification should have a broad impact in both manganese catalysis and metalloradical chemistry.

Online content

Any methods, additional references, Nature Research reporting summaries, source data, extended data, supplementary information, acknowledgements, peer review information; details of author contributions and competing interests; and statements of data and code availability are available at https://doi.org/10.1038/s41557-020-00589-8.

Received: 17 July 2019; Accepted: 21 October 2020;
Published online: 14 December 2020

References

1. Troegel, D. & Stohrer, J. Recent advances and actual challenges in late transition metal catalyzed hydrosilylation of olefins from an industrial point of view. *Coord. Chem. Rev.* **255**, 1440–1459 (2011).
2. Hill, R. M. (ed.) in *Silicone Surfactants*, *Surfactants Science Series* Vol. 86 (Marcel Dekker, 1999).
3. Franz, A. K. & Wilson, S. O. Organosilicon molecules with medicinal applications. *J. Med. Chem.* **56**, 388–405 (2013).
4. Sore, H. F., Gallowaya, W. & Spring, D. R. Palladium-catalysed cross-coupling of organosilicon reagents. *Chem. Soc. Rev.* **41**, 1845–1866 (2012).
5. Sanchez, C., Belleville, P., Popall, M. & Nicole, L. Applications of advanced hybrid organic–inorganic nanomaterials: from laboratory to market. *Chem. Soc. Rev.* **40**, 696–753 (2011).
6. Min, G. K., Hernandez, D. & Skrydstrup, T. Efficient routes to carbon–silicon bond formation for the synthesis of silicon-containing peptides and azasilaheterocycles. *Acc. Chem. Res.* **46**, 457–470 (2013).
7. Cheng, C. & Hartwig, J. F. Catalytic silylation of unactivated C–H bonds. *Chem. Rev.* **115**, 8946–8975 (2015).
8. Bähr, S. & Oestreich, M. Electrophilic aromatic substitution with silicon electrophiles: catalytic Friedel–Crafts C−H silylation. *Angew. Chem. Int. Ed.* **56**, 52–59 (2017).
9. Corey, J. Y. Reactions of hydrosilanes with transition metal complexes and characterization of the products. *Chem. Rev.* **111**, 863–1071 (2011).
10. Marciniec, B., Maciejewski, H., Pietraszuk, C. & Pawluć, P. in *Hydrosilyaltion*: *A Comprehensive Review on Recent Advances* (ed. Marciniec, B.) (Springer, 2009).
11. Speier, J. L., Webster, J. A. & Barnes, G. H. The addition of silicon hydrides to olefinic double bonds. Part II. The use of group VIII metal catalysts. *J. Am. Chem. Soc.* **79**, 974–979 (1957).
12. Markó, I. E. et al. Selective and efficient platinum(0)-carbene complexes as hydrosilylation catalysts. *Science* **298**, 204–206 (2002).
13. Du, X. & Huang, Z. Advances in base-metal-catalyzed alkene hydrosilylation. *ACS Catal.* **7**, 1227–1243 (2017).
14. Sun, J. & Deng, L. Cobalt complex-catalyzed hydrosilylation of alkenes and alkynes. *ACS Catal.* **6**, 290–300 (2016).
15. Nakajima, Y. & Shimada, S. Hydrosilylation reaction of olefins: recent advances and perspectives. *RSC Adv.* **5**, 20603–20616 (2015).
16. Millan, A., Towns, E. & Maitlis, P. M. The direct conversion of α-olefins into vinyl- and allyl-silances catalysed by rhodium complexes. *J. Chem. Soc. Chem. Commun.* 673–674 (1981).
17. Cheng, C., Simmons, E. M. & Hartwig, J. F. Iridium-catalyzed, diastereoselective dehydrogenative silylation of terminal alkenes with $(TMSO)_2MeSiH$. *Angew. Chem. Int. Ed.* **52**, 8984–8989 (2013).
18. LaPointe, A. M., Rix, F. C. & Brookhart, M. Mechanistic studies of palladium(II)-catalyzed hydrosilation and dehydrogenative silation reactions. *J. Am. Chem. Soc.* **119**, 906–917 (1997).
19. Bokka, A. & Jeon, J. Regio- and stereoselective dehydrogenative silylation and hydrosilylation of vinylarenes catalyzed by ruthenium alkylidenes. *Org. Lett.* **18**, 5324–5327 (2016).
20. Takeuchi, R. & Yasue, H. Cationic rhodium complex-catalyzed highly selective dehydrogenative silylation of styrene. *Organometallics* **15**, 2098–2102 (1996).
21. Naumov, R. N., Itazaki, M., Kamitani, M. & Nakazawa, H. Selective dehydrogenative silylation-hydrogenation reaction of divinyldisiloxane with hydrosilane catalyzed by an iron complex. *J. Am. Chem. Soc.* **134**, 804–807 (2012).
22. Atienza, C. et al. Bis(imino)pyridine cobalt-catalyzed dehydrogenative silylation of alkenes: scope, mechanism and origins of selective allylsilane formation. *J. Am. Chem. Soc.* **136**, 12108–12118 (2014).
23. Jiang, Y., Blacque, O., Fox, T., Frech, C. M. & Berke, H. Highly selective dehydrogenative silylation of alkenes catalyzed by rhenium complexes. *Chem. Eur. J.* **15**, 2121–2128 (2009).
24. Toutov, A. A. et al. Silylation of C–H bonds in aromatic heterocycles by an earth-abundant metal catalyst. *Nature* **518**, 80–84 (2015).
25. Cheng, C. & Hartwig, J. F. Rhodium-catalyzed intermolecular C–H silylation of arenes with high steric regiocontrol. *Science* **343**, 853–857 (2014).
26. Carney, J. R., Dillon, B. R. & Thomas, S. P. Recent advances of manganese catalysis for organic synthesis. *Eur. J. Org. Chem.* 3912–3929 (2016).
27. Liu, W. & Ackermann, L. Manganese-catalyzed C–H activation. *ACS Catal.* **6**, 3743–3752 (2016).
28. Yang, X. & Wang, C. Manganese-catalyzed hydrosilylation reactions. *Chem. Asian J.* **13**, 2307–2315 (2018).
29. Pratt, S. L. & Faltynek, R. A. Hydrosilation catalysis via silylmanganese carbonyl complexes: thermal vs. photochemical activation. *J. Organomet. Chem.* **258**, C5–C8 (1983).
30. Hilal, H. S., Abu-Eid, M., Al-Subu, M. & Khalaf, S. Hydrosilylation reactions catalysed by decacarbonyldimanganese(0). *J. Mol. Catal.* **39**, 1–11 (1987).
31. Hilal, H. S., Suleiman, M. A., Jondi, W. J., Khalaf, S. & Masoud, M. M. Poly(siloxane)-supported decacarbonyldimanganese(0) catalyst for terminal olefin hydrosilylation reactions: the effect of the support on the catalyst selectivity, activity and stability. *J. Mol. Catal.* **144**, 47–59 (1999).

32. Price, J. S., Emslie, D. J. H. & Britten, J. F. Manganese silylene hydride complexes: synthesis and reactivity with ethylene to afford silene hydride complexes. *Angew. Chem. Int. Ed.* **56**, 6223–6227 (2017).
33. Carney, J. R., Dillon, B. R., Campbell, L. & Thomas, S. P. Manganese-catalyzed hydrofunctionalization of alkenes. *Angew. Chem. Int. Ed.* **57**, 10620–10624 (2018).
34. Yang, X. & Wang, C. Diverse fates of β-silyl radical under manganese catalysis: hydrosilylation and dehydrogenative silylation of alkenes. *Chin. J. Chem.* **36**, 1047–1051 (2018).
35. Mukhopadhyay, T. K., Flores, M., Groya, T. L. & Trovitch, R. J. A β-diketiminate manganese catalyst for alkene hydrosilylation: substrate scope, silicone preparation and mechanistic insight. *Chem. Sci.* **9**, 7673–7680 (2018).
36. Luo, Y. R. *Comprehensive Handbook of Chemical Bond Energies* (CRC Press, 2007).
37. Friestad, G. K. & Qin, J. Intermolecular alkyl radical addition to chiral N-acylhydrazones mediated by manganese carbonyl. *J. Am. Chem. Soc.* **123**, 9922–9923 (2001).
38. McMahon, C. M., Renn, M. S. & Alexanian, E. J. Manganese-catalyzed carboacylations of alkenes with alkyl iodides. *Org. Lett.* **18**, 4148–4150 (2016).
39. Nuhant, P. et al. Visible-light-initiated manganese catalysis for C–H alkylation of heteroarenes: applications and mechanistic studies. *Angew. Chem. Int. Ed.* **56**, 15309–15313 (2017).
40. Wang, L., Lear, J. M., Rafferty, S. M., Fosu, S. C. & Nagib, D. A. Ketyl radical reactivity via atom transfer catalysis. *Science* **362**, 225–229 (2018).
41. Yang, X. & Wang, C. Dichotomy of manganese catalysis via organometallic or radical mechanism: stereodivergent hydrosilylation of alkynes. *Angew. Chem. Int. Ed.* **57**, 923–928 (2018).
42. Herrick, R. S., Herrinton, T. R., Walker, H. W. & Brown, T. L. Rates of halogen atom transfer to manganese carbonyl radicals. *Organometallics* **4**, 42–45 (1985).
43. Docherty, J. H., Peng, J., Dominey, A. P. & Thomas, S. P. Activation and discovery of earth-abundant metal catalysts using sodium *tert*-butoxide. *Nat. Chem.* **9**, 595–600 (2017).
44. Hicks, J. D., Hyde, A. M., Cuezva, A. M. & Buchwald, S. L. Pd-catalyzed *N*-arylation of secondary acyclic amides: catalyst development, scope and computational study. *J. Am. Chem. Soc.* **131**, 16720–16734 (2009).
45. Fischer, H. The persistent radical effect: a principle for selective radical reactions and living radical polymerizations. *Chem. Rev.* **101**, 3581–3610 (2000).
46. Leifert, D. & Studer, A. The persistent radical effect in organic synthesis. *Angew. Chem. Int. Ed.* **59**, 74–108 (2020).
47. Martin, S. & Watson, D. A. Preparation of vinyl silyl ethers and disiloxanes via the silyl-Heck reaction of silyl ditriflates. *J. Am. Chem. Soc.* **135**, 13330–13333 (2013).
48. Denmark, S. E. & Wang, Z. Highly stereoselective hydrocarbation of terminal alkynes via Pt-catalyzed hydrosilylation/Pd-catalyzed cross-coupling reactions. *Org. Lett.* **3**, 1073–1076 (2001).
49. Oshima, K. in *Science of Synthesis* (ed. Fleming, I.) 713–754 (Thieme, 2001).
50. Whitmore, F. C. & Sommer, L. H. Organo-silicon compounds. II. Silicon analogs of neopentyl chloride and neopentyl iodide: the alpha silicon effect. *J. Am. Chem. Soc.* **68**, 481–484 (1946).
51. Obradors, C., Martinez, R. M. & Shenvi, R. A. Ph(^{i}PrO)SiH_2: an exceptional reductant for metal-catalyzed hydrogen atom transfers. *J. Am. Chem. Soc.* **138**, 4962–4971 (2016).
52. Tondreau, A. M. et al. Iron catalysts for selective anti-Markovnikov alkene hydrosilylation using tertiary silanes. *Science* **335**, 567–570 (2012).
53. Jia, X. & Huang, Z. Conversion of alkanes to linear alkylsilanes using an iridium–iron-catalysed tandem dehydrogenation-isomerization-hydrosilylation. *Nat. Chem.* **8**, 157–161 (2016).
54. Jondi, W., Zyoud, A., Mansour, W., Hussein, A. Q. & Hilal, H. S. Highly active and selective catalysts for olefin hydrosilylation reactions using metalloporphyrins intercalated in natural clays. *React. Chem. Eng.* **1**, 194–203 (2016).
55. Hu, M.-Y. et al. Ligands with 1,10-phenanthroline scaffold for highly regioselective iron-catalysed alkene hydrosilylation. *Nat. Commun.* **9**, 221 (2018).

Methods

Caution. Manganese-catalysed dehydrosilylation will produce H_2 during the reaction. The heating of sealed Schlenk tubes may be explosive, although no incidents have occurred in our laboratory. Appropriate safety precautions must be taken when undertaking the manganese-catalysed dehydrosilylation reactions reported in this Article.

General procedure for the dehydrosilylation reaction of non-gaseous alkenes. To an oven-dried 10-ml sealed tube, $[Mn_2(CO)_{10}]$ (5 mol%), ^{i}PrPNP ligand (**L12**; 10 mol%, 0.1 mmol) and $PhCF_3$ (0.2 ml) were added under air conditions and the mixture was stirred at 80 °C for 50 min to 1 h to become a deeply red homogeneous solution. Alkene (1.0 mmol) and silane (1.0 mmol) were then rapidly added, successively, into the sealed tubes with a liquid-transferring gun. The resulting yellow reaction mixture was rigorously stirred at 140 °C for 24 h. Once the reaction was finished, the solvent was removed under vacuum and the resulting residue was purified by column chromatography on silica gel to afford the products.

General procedure for the dehydrosilylation reaction of light alkenes. To an oven-dried 10-ml sealed tube, $[Mn_2(CO)_{10}]$ (5 mol%), ^{i}PrPNP ligand **L12** (10 mol%) and $PhCF_3$ (5 ml) were added. The resulting mixture was stirred at 80 °C for 50 min to 1 h to become a deeply red homogeneous solution. The mixture was then transferred to a 50-ml autoclave, the corresponding silane was added with a liquid-transferring gun, successively, and the gaseous olefin was introduced to the autoclave and displaced three times. Finally, the pressure was gradually raised to the appropriate settings, and the temperature was programmed to rise from room temperature to 115–120 °C, which was maintained for 24 h. After the reaction was finished, the solvent was removed under vacuum and the resultant residue was purified by column chromatography on silica gel to afford the products.

General procedure for the hydrosilylation reaction of non-gaseous alkenes. To an oven-dried 10-ml sealed tube, $[Mn_2(CO)_{10}]$ (3 mol%), JackiePhos ligand **L22** (6 mol%) and $PhCF_3$ (0.2 ml) were added under air and the mixture was stirred at 80 °C for 50 min to 1 h to become a yellow homogeneous solution. Alkene (1.0 mmol) and silane (1.0 mmol) were rapidly added, successively, into the sealed tubes with a liquid-transferring gun, and the resultant yellow reaction mixture was rigorously stirred at 120 °C for 24 h. After the reaction was finished, the solvent was removed under vacuum and the resultant residue was purified by column chromatography on silica gel to afford the products.

General procedure for the hydrosilylation reaction of light alkenes. To an oven-dried 10-ml sealed tube, $[Mn_2(CO)_{10}]$ (5 mol%), ligand **L21** (5 mol%) and $PhCF_3$ (5 ml) were added under air and the mixture was stirred at 80 °C for 50 min to 1 h to become a yellow homogeneous solution. The mixture was then transferred to a 50-ml autoclave, the corresponding silane was added with a liquid-transferring gun, and the gaseous olefin was introduced to the autoclave and displaced three times. Finally, the pressure was gradually raised to the appropriate settings, and the temperature was programmed to rise from room temperature to 130 °C, which was maintained for 24 h. After the reaction was finished, the solvent was removed under vacuum and the resultant residue was purified by column chromatography on silica gel to afford the products.

Data availability

All data generated or analysed during this study are included in this Article and its Supplementary Information. Crystallographic data have been deposited at the Cambridge Crystallographic Data Centre (CCDC) as CCDC 1937151 (**5**), 1937156 (**6**) and 1937154 (**19**) and can be obtained free of charge from the CCDC via www.ccdc.cam.ac.uk/getstructures.

Acknowledgements

We thank the National Natural Science Foundation of China (grants 21971108, 21971111, 21702098, 21703118, 21732003 and 21672099), the Fundamental Research Funds for the Central Universities (020514380214), the Natural Science Foundation of Jiangsu Province (grant no. BK20190006), the 'Innovation & Entrepreneurship Talents Plan' of Jiangsu Province, the 'Jiangsu Six Peak Talent Project', Shandong Provincial Natural Science Foundation (grant no. ZR2017MB038) and start-up funds from Nanjing University for financial support. Y. Liang, G. Wang and J. Han are acknowledged for their helpful suggestions and discussions. X. Wu and Y. Zhao are acknowledged for their help with H_2 liberation reactions and X-ray single-crystal structure determination. We also thank K. Liu, Z. Yan, Y. Ning and W. Li for reproducing products **3a**, **3v**, **4a** and **4m** and C. Zhu, J. Han, Y. Pang, S. Fang and W. Li for their help with the preparation of this manuscript. The DFT calculations were supported by the High Performance Computing Center of Qufu Normal University.

Author contributions

J.D., Z.Y. and J.X. conceived and designed the experiments. J.D., Z.Y. and J.M. performed the experiments. J.D. and Z.Y. analysed and discussed the experimental data. X.-A.Y. and L.M. performed DFT calculations and discussed the manuscript. J.X. wrote the manuscript with input from all authors and discussed with C.Z. All the authors have approved the final version of the manuscript.

Competing interests

The authors declare no competing interests.

Additional information

Supplementary information is available for this paper at https://doi.org/10.1038/s41557-020-00589-8.

Correspondence and requests for materials should be addressed to J.X.

Reprints and permissions information is available at www.nature.com/reprints.